

## GEOLOGICAL-GEOTECHNICAL CHARACTERIZATION OF A RESERVOIR AREA

ISABEL FERNANDES<sup>1</sup>, MARIA DOS ANJOS RIBEIRO<sup>2</sup>, JORGE NEVES<sup>3</sup>, MÁRIO QUINTA-FERREIRA<sup>4</sup>

<sup>1</sup> *Department of Geology/FCUL & IDL, Instituto Dom Luiz, Campo Grande, 1749-016 Lisbon, Portugal, mifernandes@fc.ul.pt*

<sup>2</sup> *DGAOT/FCUP, Rua do Campo Alegre, 4169-007 Porto, Portugal, maribeir@fc.up.pt*

<sup>3</sup> *EDP Produção, Rua Ofélia Diogo da Costa 39, 4149-022 Porto, Portugal, jorgepacheco.neves@edp.pt*

<sup>4</sup> *Dep. Ciências da Terra, Universidade de Coimbra. Rua Silvío Lima. 3030-790 Coimbra, Portugal, mqf@uct.uc.pt*

### Abstract

The construction of a large dam demands that an accurate study of the rock mass be performed. Besides the aspects related to the foundation, the geologic and geotechnical characteristics of the reservoir area gained increasing importance due to the possibility of slope instability which might, eventually, affect the serviceability of the dam.

Slope instability in rock masses is a complex phenomenon that can be manifested by different types of mechanisms often controlled by the geologic structure, namely the joint system. The present work presents the geological mapping performed in the area covered by the reservoir of a large dam to be built on a rock mass composed of metasedimentary rocks. To assess the stability of the reservoir slopes, the geotechnical assessment included desk study and field survey, as well as the use of digital elevation modeling (DEM) aiming to obtain a set of maps of susceptibility factors. These included the geological map of the area, altimetry, slope angle maps, slope strikes, and land use mapping complemented with stereographic projection of the joint system in different locations for kinematic analysis. The combination of susceptibility factors led to the identification of the more problematic areas.

### Keywords

metasedimentary rocks, geologic mapping, joints sets, kinematic analysis, digital elevation modeling

## 1 Introduction

The construction of a large dam is usually controversial due to several factors from the high cost of construction and river diversion to the social and environmental impacts. The construction involves several geotechnical problems in particular those related to the permeability and the mechanical properties of the rock mass foundation. However, the study of the reservoir has shown in the past to be of utmost importance as landslides in natural slopes may be induced by the increase or variation of the groundwater level or by earthquakes (Aydan, 2016). In the worst scenario, landslides in the reservoir area cause the overtopping of the dam with catastrophic consequences, as in the Vajont dam (Muller, 1964; Semenza and Ghiretti, 2000). Also, the planes of contact between different lithologies can promote the occurrence of slope failure as referred to in Ayan (2016) for the Aratozawa Dam landslide. The author explains the influence of the different mechanical properties of rocks outcropping in the area and refers to the splitting of the rocks along the bedding planes, in which mica laminations were parallel to the bedding orientation.

Following the work of Cruden (1991), and published in Fell et al (2008) landslide is defined as “the movement of a mass of rock, debris or earth down a slope”, with designations defined in Varnes (1978).

The definition of landslide susceptibility is “the quantitative or qualitative assessment of the classification, volume (or area), and spatial distribution of landslides which exist or potentially may occur in an area” (Fell et al., 2008). Regarding the factors that control the occurrence of landslides and their importance in landslide susceptibility assessment for different landslide mechanisms, a summary can be found in Corominas et al. (2014) although it seems that there is no generally agreed method for producing landslide susceptibility maps (Guzzetti et al., 2000).

The instability problems around and above the rim of the reservoir depend on several factors, namely: a) Type of soil/rock forming the slope, b) Geometry of the slope, c) Vegetation cover, and d) Human interference within the reservoir rim boundary (Anbalagan and Kumar, 2015). The assessment of the area includes, usually, the analysis of historical records, geological mapping, the study of the joints and major faults, and the evaluation of the slope stability which can be made by qualitative or quantitative methods. The inventory of landslides is traditionally performed by the visual interpretation of aerial photographs, possibly with the aid of automated methods, aiming to reduce the manual interpretation. However, information about historical records is usually scarce or not available at all. Anbalagan and Kumar (2015) state that future landslides will occur under similar conditions as past and present landslides (Lee and Talib, 2005). Pourghasemi et al. (2013) study states that the mapping of actual landslides in the study area is essential for describing the relationship between the landslide distribution and the conditioning factors. However, in the present work, there is no knowledge of multi-temporal inventories leading to the use of only the current distributional pattern to identify susceptible areas.

According to Jaedicke et al. (2014) topography is a key factor for landslide susceptibility which increases with the inclination of the slopes. The author defines different thresholds of slope angles for mass movements to occur: natural loose geological materials are stable up to slope angles of 27°; in terrain steeper than 30°, rocks and other loose materials fall continuously; and above 45°, usually only rockfalls and large rock avalanches occur.

In Pourghasemi et al. (2013) four categories of slope gradient are considered, namely: (1) 0–5°, (2) 6–15°, (3) 16–30° and (4) > 30°. In the present work, the classes in Gupta and Albalagan (1997) were followed: Escarpment/cliff (>45°), steep slope (36–45°), moderately steep slope (26–35°), gentle slope (16–25°), very gentle slope (≤15°). For the analysis, also the findings of Braathen et al. (2004) were taken into account. The authors state that in rock masses sliding can occur for slopes with angles lower than 45° and that rock falls, eventually with backstepping, take place for angles of 60–75°, in special when sub-vertical joints are present.

Regarding the elevation map, also the classes of relative relief used in Gupta and Albalagan (1997) were considered, namely: low (≤100 m), medium (101–300 m), and high (>300 m).

By the end of 2000’s first decade, studies were developed to evaluate the viability of a large dam in the centre of Portugal equipped with a hydraulic tunnel and an underground power plant. The dam site is located in an asymmetric V-shaped valley with the abutment on the left bank steeper than the right bank. The dam is planned to be a roller-compacted concrete gravity dam with 89 m maximum height, and 400 m width at its crest.

The present work summarizes the results obtained by the geological-geotechnical assessment of the reservoir covering an area of about 70 km<sup>2</sup> and presents the methods used for the preliminary assessment of the stability of slopes around and above the rim of the reservoir.

## 2 Methods

The geological-geotechnical study of the area affected by the reservoir involved the combination of different methodologies to assess the stability of the reservoir slopes: a) in-situ investigation of mass movements and historical inventory; b) analysis of aerial photographs and satellite images with draft of the structural map of the area; c) production of the geological map based on field survey; d) production of thematic maps of the triggering factors (altimetry, slope angle maps, and slope strikes), using digital elevation modeling (DEM); e) land use mapping; f) stereographic projection of the joint system in a different location to perform the kinematic analysis.

The characterization of the area, with the predominant orientation of the river of NNE-SSW, included a preliminary desk study in which all the available maps for the region were collated and orthophoto maps analyzed. Aerial photographs on 1:6,667 scale were observed to define the structure of the rock mass

and to identify the main faults and tectonic alignments; register historic landslide scars; and delineate the roads and paths to be used during the field survey.

The field survey included extensive mapping at the scale 1:10,000 of the area covered and surrounding the future reservoir and the establishment of joint survey stations. The recommendations in ISRM (1979) were followed in what concerns the characteristics of the joints, namely, the dip/dip direction, spacing, aperture, persistence, and roughness. The rock mass was classified according to the degree of weathering (W1 to W5) and fracturing (F1 to F5). The dip/dip direction data were plotted on a stereonet projection using the software DIPS (Rocscience) to define the main sets of joints and to prepare histograms for each characteristic assessed. The roughness of each discontinuity was evaluated by comparison with roughness profiles to attribute a JCR value.

### 3 Results

#### 3.1 Historic record

The study area has a low density of population concentrated in small villages with most of the area uninhabited. In consequence, the possible effects of landslides on the property and the few occurrences have not been registered. To prepare the landslide inventory map, the aerial photograph and the satellite images were analyzed and orthophotographic maps were interpreted. The information about past landslides was complemented during the field survey for geological mapping. The observation in situ allowed the identification of very small volume mass movements related to the manmade walls for agricultural use and the accumulation of debris at the river banks in restricted areas (Figure 1).



Figure 1. Mass movement features interesting very restricted areas

#### 3.2 Morphology and land use

The fluvial network follows the main structural alignments in the region, namely NE-SW and N-S. The valley walls contain rare terracing as well as alluvial deposits plains. The hills show flattened summit surfaces. The area is characterized by very low population density (7.8 to 11 inhabitants per km<sup>2</sup>). The small villages are situated at the top of the hills, far from the rim surrounding the reservoir, which will have its maximum water level at 227 m elevation.

The geomorphology of the area shows smooth slopes and occasional cliffs, relief variation from 100 to 300 m, and a low longitudinal profile. Vegetation covers most of the valleys and hills in the wide valley extending for 24 km along the river and tributaries. The dense fluvial network defines a rectangular drainage pattern with some entrenched meanders, in which the steepest cliffs are observed.

The slopes are steeper close to the confluence of the main river and the two larger tributaries. The observation of the slope angle map shows that the slopes have dominantly angles <25°. Slopes >45° are scarce and occur in restricted areas, more commonly close to the meanders of the river. In Figure 2 two areas of the reservoir are shown to exemplify the topography and inclination of the river banks.

In the area, the land use is divided between agricultural land and fallow land. There used to be olive-rich agriculture but with the aging of inhabitants and desertification, most of these are now abandoned. They were arranged in terraces along the slopes, limited by ancient armor stone walls. The recent agriculture terraces with olives are more abundant in the NW bank of the river, dipping to S and SE. The most recent agricultural use is dedicated to eucalyptus which is planted at higher elevations on the

river banks, in special where the morphology becomes smoother. It is more common in the upstream extremity of the reservoir. The outcrops of rock are more common on the SE bank of the river, coinciding with the slopes oriented to N and NW.

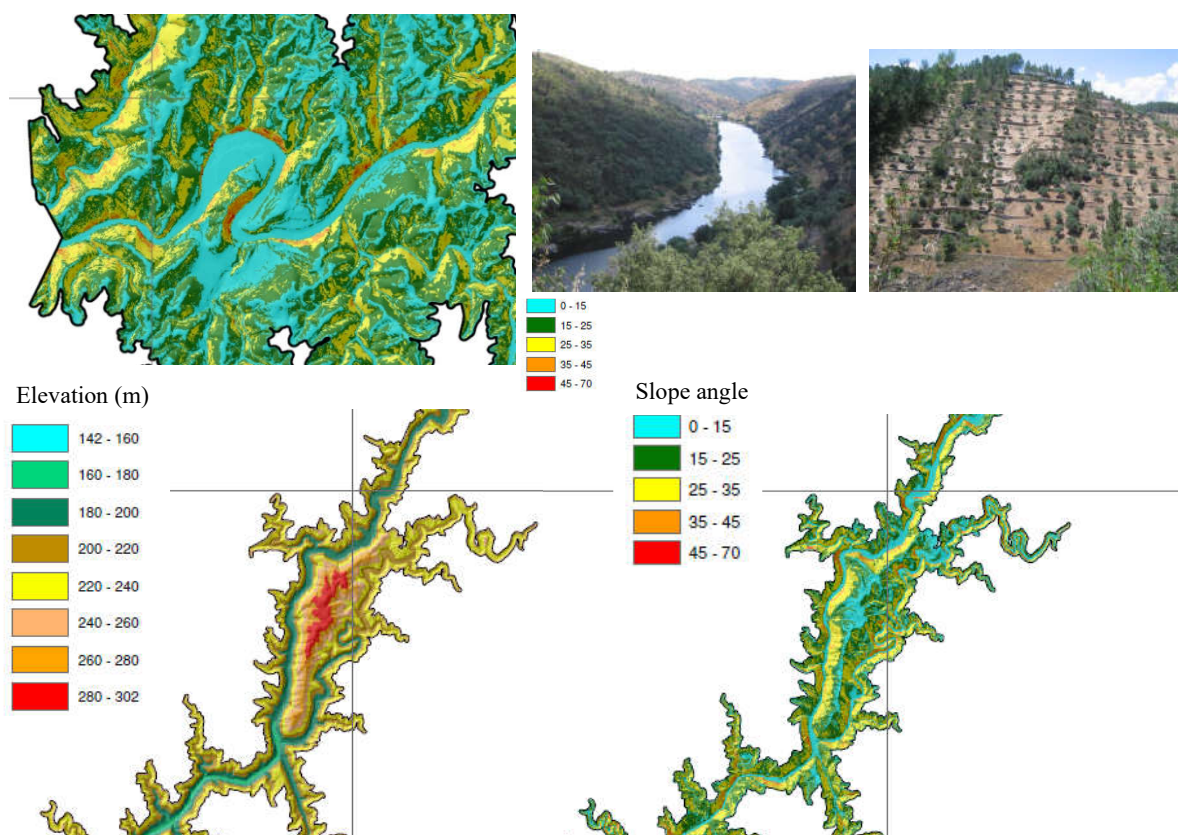


**Figure 2.** Aspects of the geomorphology of the valley, showing dominantly smooth slopes ( $<20^\circ$ ): the area of the larger meander, located 2 km upstream of the dam site, the highest elevation area, and examples of the land use

### 3.3 Geologic mapping of the reservoir

In the area, a sequence of metasedimentary rocks outcrops formed by layers of variable thickness of metagreywacke (quartz-rich rock) and phyllite. This formation outcrops in a wide area of the country and is named the Schist-Greywacke Complex (SGC) (Medina et al., 1998; Pereira et al., 2012). The works published about the rock mass of the area of study refer to the Beiras Group of the Schist-Greywacke Complex dated from the late Proterozoic to the Cambrian period which is composed of metasedimentary rocks of the greenschist facies, in the chlorite zone and, locally, in the biotite zone. Some small areas of fluvial terraces occur along the river banks. They contain conglomeratic deposits with an abundant matrix of ferruginous sandy clay and are 2 to 3 m in height.

Along the area, three slightly different formations were found, namely Perais, Malpica, and Rosmanihal. All these formations were affected by the Variscan orogeny which imposed folding and low-grade metamorphic features. The geological contacts are aligned NE-SW to WNW-ESE.

Rosmanihal formation outcrops in the upper part of the reservoir area, where the valley is wider and the slopes smoother. It is characterized by the dominance of pelitic layers with some millimetric to centimetric layers of metagraywacke and rare conglomerate intercalations.

The Malpica formation is the basal unit of the SGC. It occupies a narrow part of the reservoir, coinciding with the highest elevation and steeper slopes in the area. It is characterized by the predominance of metagreywacke with minor phyllite intercalations.

Perais formation occurs in the dam emplacement site and is composed of thin layers of turbiditic meta-siltite and meta-argillite and centimetric to decimetric layers of meta-greywacke.

At the surface, the rock mass is weathered to heavy weathered (W3 to W4), mainly in the phyllite layers,

and shows close to very close joints (F4-F5). Foliation, the main anisotropic feature of the rock mass, defines very small blocks that tend to produce localized rock fall and toppling. Drill cores obtained for the study of the dam foundation rock mass show that the rocks are dark grey to black in color when sound (W1), and moderately spaced (F3). In the quartz-rich layers, the foliation is not well marked whilst in the phyllite it imprints a strong anisotropy to the rock. The surficial soil forms a thin layer mainly composed of clay. Figure 3 presents the main aspects of the three formations and the surficial soil.

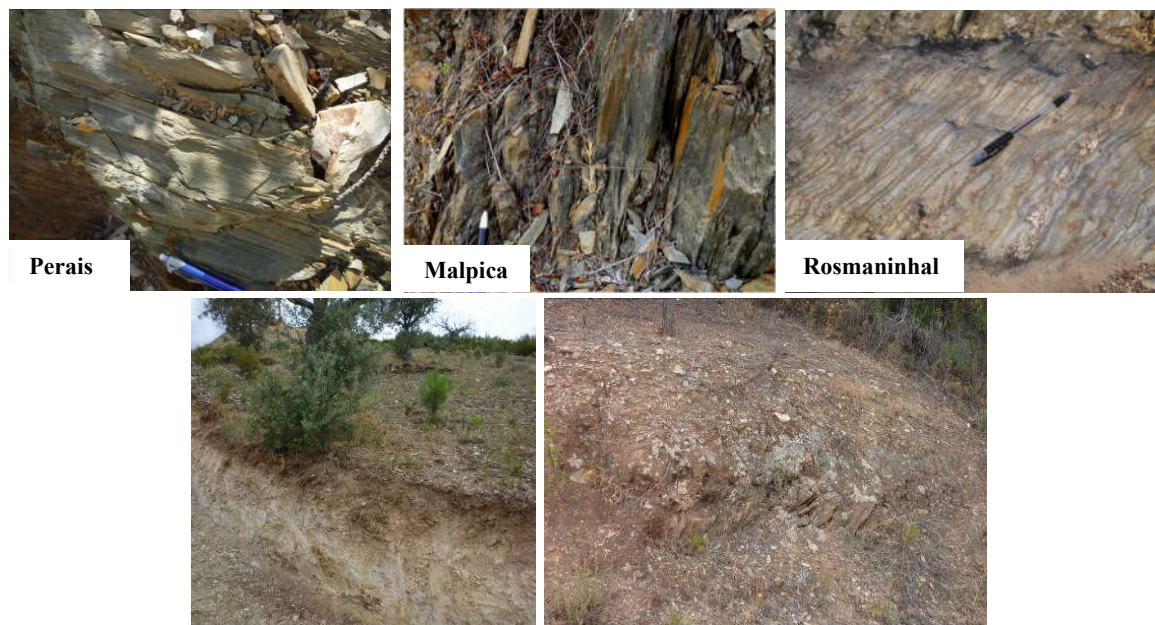


**Figure 3.** General features of the three geological formations identified and of the surficial soils. The thin surface soil is composed of poor quality highly weathered rock, silt, and clay.

### 3.4 Structure and geomechanical characteristics

The main alignments were identified by the analysis of the aerial photographs and Google Earth, and plotted on the topographic map to prepare the fieldwork. The outcrops are rare and the places to assess the rock mass structure are limited. The choice was conditioned to the locations where enough measurements (tens) could be made. At the surface, the rock mass is heavily cracked by the foliation planes which are open due to weathering, giving place to tiny blocks of rock which cause small-scale rock falls.

The foliation is oriented NW-SE, parallel to the stratification, which agrees with the regional alignments (Figure 4). It constitutes the main set of discontinuities in the three formations outcropping. Besides this NW-SE sub-vertical set, there are subhorizontal joints that define centimetric blocks of rock by the intersection with the main set. The regional fractures also include ENE-WSW to NE-SW and N-S to NNE-SSW. The major faults are NE-SW, sub-vertical and many of the rivers and tributaries follow the sub-vertical faults alignments. The quartz veins are usually associated with the faults and the fault gauge is formed of fragments of rock, intensely tectonized quartz, clay, and iron oxides.

The section of the valley closer to the dam site is oriented E-W to ENE-WSW and shows a narrow meander with steep slopes, influenced by a major fault parallel to the valley. Upstream, NW-SE faults are dominant, which is approximately perpendicular to the NE-SW valley orientation.

Table 1 presents the characteristics of the main faults identified during the fieldwork performed for the geologic mapping.

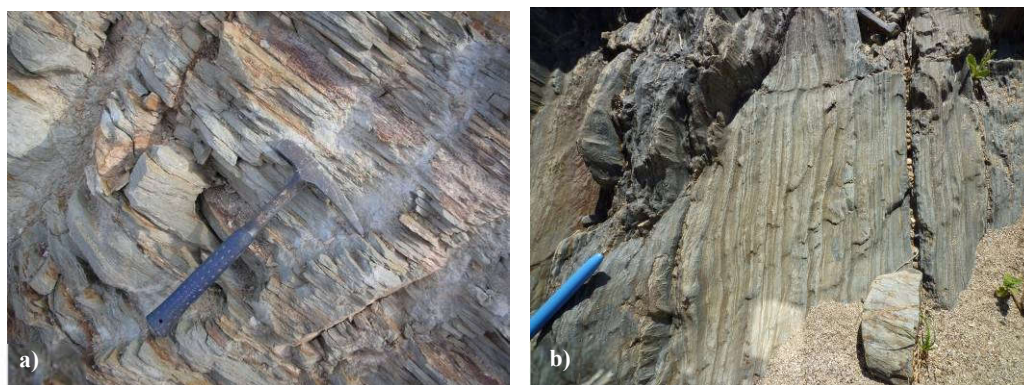


**Figure 4.** Perais formation, close to the dam site, composed of grey phyllite and greywacke thin layers, S0/S1: N150°; 60°SW to N140°; 80°SW

**Table 1.** Characteristics of the main faults mapped in the area

Fault	Orientation	Gauge (m)	Description of the fault gouge
A	N110°; 90°	4,5	Fragments of quartz and schist with clay
B	N60°; 80°W	6,5	Fragments of quartz and schist with clay
C	N0°; 90°	4,0	Fragments of quartz and schist with clay; several fractures parallel
D	N35°; 90°	4,0	Ferruginous fragments of quartz and schist with clay;
E	N0°; 90°	5,0	Fragments of quartz and schist
F	N45° a 50°; 90°	10,0	Brecciated fault gouge
G	N135°; 65°SW	9,0	Fragments of quartz with clay
H	N115°; 90°	5,0	Fragments of quartz and schist with clay

The metasedimentary rocks that form the rock mass both of the dam foundation and the reservoir were characterized by laboratory tests elsewhere (Loureiro et al., 2014; Quinta Ferreira et al., 2015). The values obtained for the sound velocity ( $V_p$ ) of un-weathered rock cores vary from as low as 561 m/s, for the phyllite layers, to 3378 m/s, for the quartz-rich layers, with an average of 1657 m/s. The unconfined strength ranges from 4 to 78 MPa, being lower for the phyllite layers than for the quartz-rich layers (meta-greywacke). The drill cores, however, mostly show the axis subparallel to the foliation, which may affect the results of the UCS tests.

Regarding the visual characterization of the rock mass *in situ*, the values of GSI are 30-45 for the phyllite layers and 40-55 for the quartz-rich layers, assuming 30 and 40 as the worst scenario, respectively, and  $m_i$  of 10. Table 2 shows the mechanical parameters of the rock mass obtained using Hoek-Brown et al. criterion (2002) for a slope of 30 m maximum height, which seldom occurs and assumes the worst scenario for the value of GSI.

**Table 2.** Properties of the rock mass based on GSI analysis and laboratory test results (using RSdata software)

	Phyllite layers	Quartz-rich layers (Meta-greywacke)
UCS (MPa)	31	48
GSI	30	40
$m_i$	10	10
E (MPa)	880	1948
Cohesion (MPa)	0.080	0.146
$\phi$ (°)	23	33

### 3.4 Kinematic analysis

The results obtained with DIPS software defined the main sets of discontinuities. The kinematic analysis included the assessment of four types of mass movements: planar sliding, wedge sliding, and direct and

flexural toppling (Hudson and Harrison, 1995). The analysis was carried out considering the possibility of having a slope of 60°, which constitutes the worst possible scenario, and a friction angle of 30°. Table 3 summarizes the results of the kinematic analysis for each formation using the main orientations of the valley for each formation.

The results obtained confirm the site observation that the main mass movement is due to direct toppling and flexural toppling. These movements may occur at the lower levels of the river banks, where the river excavated steep slopes, and in the manmade excavations for agriculture. The sub-vertical foliation causes the toppling but the dimensions of the blocks are smaller than 50 cm due to the intense fracturing of the rock mass at the surface. The foliation planes and the joints are smooth and show iron oxides due to water percolation and exposition to the weathering elements.

**Table 3.** Evaluation of the different types of mass movements (%) obtained by kinematic analysis (DIPs)

	Valley	Planar sliding	Wedge sliding	Direct toppling	Flexural toppling
<b>Rosmaninhal</b>	N-S, 60°E	0	4	8	0
	N-S, 60°W	6	12	100 (set 2)	2
	N20°, 60°SE	0	4	10 (oblique)	93 (set 1)
	N20°, 60°NW	2	14	94 (set 2)	0
	N120°, 60°NE	0	0	1	6
	N120°, 60°SW	3	3	94 (set 2)	93 (set 1)
<b>Malpica</b>	N-S, 60°E	1	18	6	0
	N-S, 60°W	0	9	75 (set 2)	0
	N30°, 60°SE	3	19	7	6
	N30°, 60°NW	32 (set 2)	14	100 (set 2)	0
<b>Perais</b>	N-S, 60°E	0	3	42 (set 2)	0
	N-S, 60°W	0	3	70 (set 2)	12
	N40°, 60°SE	0	4	12	0
	N40°, 60°NW	0	5	87 (set 2)	100 (set 3)

#### 4 Conclusion

A field survey was carried out to elaborate the geological mapping of the area. The lithology is similar in all the area covered by the reservoir. The river and tributaries have a smooth longitudinal profile. The river flows in a V-valley with rare alluvial deposits.

The structure of the rock mass was assessed to map the main faults and to define the joint sets. Foliation is the main feature, mainly sub-vertical. It is parallel to the stratigraphic contacts (S0//S1) between materials that vary from very fine-grained phyllites to medium-grained quartz-meta-greywackes. The mechanical characteristics of both lithologies are different but the layers are very thin and limits cannot be defined at the scale of the study.

The definition of the joint sets and the use of kinematic analysis performed allow to understand that toppling is the most probable type of mass movement. As observed in the fieldwork, there are localized manifestations of toppling due to the dip/dip direction of the schistosity. However, the spacing of the fractures defines small blocks (F4-F5) which are visible at the lower levels of the river banks and along excavations prepared for agriculture.

#### Acknowledgments

This work was funded by the Portuguese Fundação para a Ciência e a Tecnologia (FCT) I.P./MCTES through national funds (PIDDAC) – UIDB/50019/2020 (<https://doi.org/10.54499/UIDB/50019/2020>), UIDP/50019/2020 (<https://doi.org/10.54499/UIDP/50019/2020>) and LA/P/0068/2020 (<https://doi.org/10.54499/LA/P/0068/2020>).

#### References

Anbalagan, R.; Kumar, R. Reservoir induced landslides –A case study of reservoir rim region of Tehri Dam. *TIFAC-IDRIM Conference* 28th –30th October 2015 New Delhi, India, 2015.

- Aydan, O. Some considerations on a large landslide at the left bank of the Aratozawa Dam caused by the 2008 Iwate–Miyagi intraplate earthquake. *Rock Mech Rock Eng*, 2016, 49, 2525–2539. DOI 10.1007/s00603-016-0977-1
- Corominas, J.; van Westen, C.; Frattini, P.; Cascini, L.; Malet, J.-P.; Fotopoulou, S.; Catani, F.; van Den Eeckhaut, M.; Mavrouli, O.; Agliardi, F.; Pitolakis, K.; Winter, M. G.; Pastor, M.; Ferlisi, S.; Tofani, V.; Herva's, J.; Smith J. T. (2014). Recommendations for the quantitative analysis of landslide risk. *Bull Eng Geol Environ*. 2014, 73, 209–263.
- Cruden, D.M. A simple definition of a landslide, *Bulletin of the International Association of Engineering Geology*, 1991, 43, 27-29.
- Gupta, P.; Anbalagan, R. Slope stability of Tehri Dam Reservoir Area, India, using landslide hazard zonation (LHZ) mapping, *Quarterly Journal of Engineering Geology and Hydrogeology*, 1997, 30 (1): 27–36. <https://doi.org/10.1144/GSL.QJEGH.1997.030.P1.03>
- Guzzetti, F.; Cardinali, M.; Reichenbach, P.; Carrara, A. Comparing Landslides Maps: A case study in the Upper Tiber Basin, Central Italy, *Environmental Management*. 2000, 25/ 3, 247-263.
- Hoek. E.; Carranza-Torres, C.; Corkum, B. Hoek-Brown failure criterion-2002 edition, in *Proc. The 5th North American Rock Mechanics Symp*, Toronto, Canada. 2002, 1, 267-273.
- ISRM. Suggested Methods for the Quantitative Description of Discontinuities in Rock Masses, *Int. J. Rock Mech. Min. Sci. & Geomech. Abstr.*, 1979, 15, 319-368.
- Jaedicke, C.; Van Den Eeckhaut, M.; Nadim, F. et al. Identification of landslide hazard and risk 'hotspots' in Europe. *Bull Eng Geol Environ*, 2014, 73, 325–339. <https://doi.org/10.1007/s10064-013-0541-0>
- Lee, S.; Talib, J. A. Probabilistic landslide susceptibility and factor effect analysis. *Environ. Geol.*, 2005, 47, 982-990.
- Loureiro, F.; Fernandes, I.; Ribeiro, M. A; Neves, J.; Quinta-Ferreira, M. Characterization of a schist using laboratory tests. *SGEM*, Albena, Bulgaria, 2015, 1(2):171-178.
- Medina, J.; Sequeira, A.; Silva, F.; Oliveira, J.T.; Rodriguez Alonso, M.D. O complexo Xisto-Grauváquico (CXG) da região de V.N. de Poiares-Arganil- Mortagua. In: Oliveira, J.T., Dias, R.P. (Eds.), Livro Guia das Excursões, *V Congresso Nacional de Geologia*. Lisboa, Portugal. 1998, 137–158.
- Muller, L. The rock slide in the Vaiont Valley. *Rock Mech Eng, Geol*, 1964, 2, 148–212.
- Pereira, M.F.; Linnemann, U.; Hofmann, M.; Chichorro, M.; Solá, A.R.; Medina, J.; Silva; J.B. The provenance of Late Ediacaran and Early Ordovician siliciclastic rocks in the Southwest Central Iberian Zone: Constraints from detrital zircon data on northern Gondwana margin evolution during the late Neoproterozoic. *Precambrian Research*, 2012, 166– 189.
- Pourghasemi, H. R.; Goli Jirandeh, A.; Pradhan, B.; Xu, C.; Gokceoglu, C. Landslide susceptibility mapping using support vector machine and GIS. *J. Earth Syst. Sci.*, 2013, 122: 349–369.
- Fell, R.; Corominas, J.; Bonnard, C.; Cascini, L.; Leroi, E.; Savage, W.Z. *Guidelines for landslide susceptibility, hazard and risk zoning for land use planning*, on behalf of the JTC-1 Joint Technical Committee on Landslides and Engineered Slopes. 2008a, 102, Issues 3–4, 85-98.
- Quinta-Ferreira, M., Fernandes, I., Loureiro, F., Alves, J., Perdigão, R., Ribeiro, M.A., Santarém Andrade, P., Neves, J. Geologia de Engenharia de rochas xistosas: os xistos negros da EN17 em Coimbra e os filitos de Vila Velha de Ródão. *Comunicações Geológicas*, 2015, 12/102, Issue 1, 89-96, *Atas do VIII Seminário Recursos Geológicos, Ambiente e Ordenamento do Território*, UTAD, Vila Real. DOI: 10.13140/RG.2.1.2214.8569.
- Semenza, E.; Ghirotti, M. History of the 1963 Vaiont slide: the importance of geological factors. *Bull Eng Geol Environ*, 2000, 59, 87–97
- Varnes, D. J. *Slope Movement Types and Processes*, In: Landslides Analysis and Control, (Ed. R.L. Schuster and R.J. Krizek), Transportation Research Board, National Academy of Sciences, Special Report, 1978, 176, 12-33.